

Observations of the pulsating subdwarf B star Feige 48: Constraints on evolution and companions

M. D. Reed,^{1*}† S. D. Kawaler,² S. Zola,³ X. J. Jiang,⁴ S. Dreizler,^{5,6} S. L. Schuh,⁵ J. L. Deetjen,⁵ R. Kalytis,⁷ E. Meištas,⁷ R. Janulis,⁸ D. Ališauskas,⁷ J. Krzesiński,^{9,10} M. Vuckovic,² P. Moskalik,¹¹ W. Ogloza,⁹ A. Baran,⁹ G. Stachowski,^{3,9} D. W. Kurtz,¹² J. M. González Pérez,¹³ A. Mukadam,¹⁴ T. K. Watson,¹⁵ C. Koen,^{14,16} P. A. Bradley,¹⁷ M. S. Cunha,^{18,19} M. Kilic,¹⁴ E. W. Klumpe,²⁰ R. F. Carlton,²⁰ G. Handler,^{16‡} D. Kilkenny,¹⁶ R. Riddle,² N. Dolez,²¹ G. Vauclair,²¹ M. Chevreton,²² M. A. Wood,²³ A. Grauer,²⁴ G. Bromage,¹² J. E. Solheim,¹³ R. Østensen,²⁵ A. Ulla,²⁶ M. Burleigh,²⁷ S. Good,²⁷ Ö. Hürkal,²⁸ R. Anderson²⁹ and E. Pakstiene⁸

¹Department of Physics, Astronomy and Material Science, Southwest Missouri State University, 901 S. National, Springfield, MO 65804 USA

²Department of Physics and Astronomy, Iowa State University, Ames, IA 50011 USA

³Astronomical Observatory, Jagiellonian University, ul. Orla 171, 30-244, Cracow, Poland

⁴National Astronomical Observatories, Chinese Academy of Sciences, Beijing, 100012, PR China

⁵Institut für Astronomie und Astrophysik, Universität Tübingen, Sand 1, D-72076, Tübingen, Germany

⁶Universitäts-Sternwarte Göttingen, Georg-August-Universität Göttingen, Geismarlandstraße 11, D-37083 Göttingen, Germany

⁷Institute of Material Science and Applied Research of Vilnius University, Astronomical Observatory, Ciurlionio 29, Vilnius LT-2009, Lithuania

⁸Institute of Theoretical Physics and Astronomy, Astronomical Observatory, Goštauto 12, Vilnius LT-2600, Lithuania

⁹Mt. Suhora Observatory, Crakow Pedagogical University, ul. Podchorążych 2, PL-30-084 Cracow, Poland

¹⁰Apache Point Observatory, PO Box 59, Sunspot, NM 88349, USA

¹¹Nicolas Copernicus Astronomical Centre, Polish Academy of Sciences, ul. Bartycka 18, 00-716 Warsaw, Poland

¹²Centre for Astrophysics, University of Central Lancashire, Preston PR1 2HE

¹³Institutt for Fysikk, Universitet i Tromsø, N-9037 Tromsø, Norway

¹⁴Department of Astronomy, University of Texas, Austin, TX 78712, USA

¹⁵Southwestern University, 1001 E. University Avenue, Georgetown, TX 78626, USA

¹⁶South African Astronomical Observatory, PO Box 9, Observatory 7935, Cape, South Africa

¹⁷Los Alamos National Laboratory, X-2, MS T-085, Los Alamos, NM 87545, USA

¹⁸Centro de Astrofísica da Universidade do Porto, Rua das Estrelas, 4150-762 Porto, Portugal

¹⁹Instituto Superior da Maia, Av. Carlos de Oliveira Campos, 4475-690, Avisoso S. Pedro, Castelo da Maia, Portugal

²⁰Middle Tennessee State University, Department of Physics and Astronomy, Murfreesboro, TN 37132, USA

²¹Université Paul Sabatier, Observatoire Midi-Pyrénées, 14 Avenue E. Belin, 31400 Toulouse, France

²²Observatoire de Paris-Meudon, DAEC, 92195, Meudon, France

²³Department of Physics and Space Sciences & SARA Observatory, Florida Institute of Technology, Melbourne, FL 32901-6975, USA

²⁴Department of Physics and Astronomy, University of Arkansas at Little Rock, Little Rock, AR 72204, USA

²⁵Isaac Newton Group of Telescopes, E-37800 Santa Cruz de La Palma, Canary Islands, Spain

²⁶Universidade de Vigo, Depto. de Física Aplicada, Facultade de Ciencias, Campus Marcosende-Lagoas, 36200 Vigo, Spain

²⁷Department of Physics and Astronomy, University of Leicester, Leicester LE1 7RH, England

²⁸Ege University, Science Faculty, Department of Astronomy and Space Sciences, Bornova 35100 Izmir, Turkey

²⁹Department of Physics and Astronomy, University of North Carolina, Chapel Hill, NC 27599-3255, USA

Accepted 2003 November 15. Received 2003 November 10; in original form 2002 November 14

ABSTRACT

Since pulsating subdwarf B (sdBV or EC14026) stars were first discovered, observational efforts have tried to realize their potential for constraining the interior physics of extreme horizontal branch stars. Difficulties encountered along the way include uncertain mode identifications and a lack of stable pulsation mode properties. Here we report on Feige 48, an sdBV

*E-mail: mreed@sdbv.smsu.edu

†Visiting astronomer, McDonald and Fick Observatories.

‡Present address: Institut für Astronomie, Universität Wien, Türkenschanzstraße 17, A-1180 Wien, Austria.

star for which follow-up observations have been obtained spanning more than four years. These observations show some stable pulsation modes.

We resolve the temporal spectrum into five stable pulsation periods in the range 340–380 s with amplitudes less than 1 per cent, and two additional periods that appear in one data set each. The three largest amplitude periodicities are nearly equally spaced, and we explore the consequences of identifying them as a rotationally split $\ell = 1$ triplet by consulting a representative stellar model.

The general stability of the pulsation amplitudes and phases allows us to use the pulsation phases to constrain the time-scale of evolution for this sdBV star. Additionally, we are able to place interesting limits on any stellar or planetary companion to Feige 48.

Key words: stars: individual (Feige 48) – stars: oscillations – stars: variables: other.

1 INTRODUCTION

To date, over 30 pulsating subdwarf B (EC 14026 or sdBV) stars have been identified, with pulsation periods ranging from 68 to 528 s and with amplitudes generally less than 50 millimagnitudes (mmag). For recent reviews of this class of stars, see Kilkenny (2001), and for observational properties, see Reed, Kawaler & Kleinman (2000), and references therein Charpinet, Fontaine & Brassard (2001, and references therein) describe in detail some important aspects of pulsation theory in sdB stars. Most sdBV stars show periods at the short end of the range, and probably represent stars close to the zero-age horizontal branch (ZAHB). PG 1605+072 is the longest-period, and lowest-gravity, sdBV star, with Feige 48 being an intermediate object. In general, the longer-period sdBV stars represent more highly evolved objects.

Feige 48 was identified as a ‘faint blue star’ as part of the Feige survey (Feige 1958). It was recategorized as an sdB star when it was observed as part of the Palomar–Green survey (Green, Schmidt & Liebert 1986). Koen et al. (1998, hereafter K98) identified five pulsation periods in Feige 48 in six observing runs from 1997 May to 1998 February. The periods detected by K98 range from 342 to 379 s with the largest amplitude being 6.4 mmag. Amplitude variability led K98 to conclude that mode beating was probably present, implying that other unresolved modes were present in their data. This provided the motivation for our follow-up observations. Heber, Reid & Werner (1999; hereafter HRW) obtained a high-resolution (0.09 Å) spectrum of Feige 48, from which they determined $\log g = 5.50 \pm 0.05$ and $T_{\text{eff}} = 29\,500 \pm 300$ K. This places Feige 48 among the coolest sdBV stars known, with a surface gravity intermediate between PG 1605+072 and the rest of the class.

Here we report on our multi-year campaign of high-speed photometry of Feige 48. In Section 2, we outline our observations. Section 3 describes the time series analysis and period identifications. We report on a stellar model fit to Feige 48 in Section 4. The phase stability of pulsations is described in Section 5, where we use this stability to place interesting limits on any possible planetary companion. Section 6 gives our conclusions and outlines future observations for Feige 48.

2 HIGH-SPEED PHOTOMETRY

We began observing Feige 48 in 1998 November, and our most recent observations were acquired in 2002 May. Table 1 provides

a complete list of our observations (including the observations of K98). We acquired most of the data using three-channel photoelectric photometers as described in Kleinman, Nather & Phillips (1996). At Fick Observatory, we used a two-channel photometer of similar design. The Fick data typically have a ≈ 30 -min gap during the night, as the telescope mount requires the photometer to be disconnected when the telescope exchanges sides on the pier. Because this instrument is a two-channel photometer, the data were occasionally interrupted to measure the sky background. All photometers used Hamamatsu R647 photomultiplier tubes. Data acquired at Calar Alto and SARA were obtained using CCDs with 5-s exposures on a 30- and 15-s duty cycle, respectively. As both the target and comparison star were in the same CCD field, differential photometry removed extinction and sky variation. However, since extinction is wavelength-dependent, colour differences between the stars produced small non-linear trends in the data. We remove these trends by dividing by a low-order (2–4) polynomial fitted to the single-night data. Bad points in the CCD data were removed by hand. No filters were used during any of the photoelectric observations to maximize the photon count rate, whereas the CCD observations used filters to approximate the passband of the Hamamatsu phototubes (Kanaan et al. 2000).

As Table 1 indicates, we have obtained a total of ≈ 380 h of time-series photometry on Feige 48. The data span from 1998 January to 2002 May (the two runs in 1997 were too short and too temporally separated to be useful for this analysis).

3 THE PULSATION SPECTRUM OF FEIGE 48

We follow the standard procedure for determining pulsation frequencies from time-series photometry obtained using the Whole Earth Telescope (see, for example, O’Brien et al. 1998). In short, we identify the principal pulsation frequencies with a Fourier transform (FT) of light curves of individual nights. We then combine data from several contiguous nights to refine the frequencies. Once the main frequencies are found, we then do a non-linear least-squares fit for the frequencies, amplitudes and phases of all identified peaks, along with their uncertainties.

To work around monthly and annual gaps between observing runs, we begin our analysis of the data in separate, relatively contiguous subgroups. The dates and data hours obtained for the subgroups are given in Table 2, and the temporal spectra and window functions for the groups are plotted in Fig. 1. All groups were analysed

Table 1. Observations of Feige 48.

Run	Length (h)	Date UT	Observatory	Run	Length (h)	Date UT	Observatory
tex-007	1.2	1997.03.05	McDonald 0.9 m	suh-106	3.2	2000.08.11	Suhora 0.6 m
tex-018	2.1	1997.02.06	McDonald 0.9 m	jsx-125	2.5	2000.26.11	BAO 0.85 m
tex-223	5.7	1998.23.01	McDonald 0.9 m	jsx-128	3.2	2000.27.11	BAO 0.85 m
tex-236	2.9	1998.28.01	McDonald 0.9 m	suh-107	8.8	2000.21.12	Suhora 0.6 m
tex-239	5.5	1998.29.01	McDonald 0.9 m	suh-108	3.4	2000.22.12	Suhora 0.6 m
tex-241	5.9	1998.30.01	McDonald 0.9 m	mdr145	8.0	2001.18.01	Fick 0.6 m
tex-246	6.7	1998.01.02	McDonald 0.9 m	mdr146	8.2	2001.20.01	Fick 0.6 m
mdr006	2.2	1998.22.11	McDonald 0.9 m	mdr147	3.6	2001.21.01	Fick 0.6 m
mdr009	2.6	1998.23.11	McDonald 0.9 m	mdr148	9.2	2001.22.01	Fick 0.6 m
mdr012	2.6	1998.24.11	McDonald 0.9 m	mdr149	9.5	2001.24.01	Fick 0.6 m
mdr017	2.8	1998.26.11	McDonald 0.9 m	mdr150	9.2	2001.25.01	Fick 0.6 m
mdr018	6.0	1999.06.03	McDonald 2.1 m	mdr151	7.3	2001.01.02	Fick 0.6 m
mdr021	5.5	1999.09.03	McDonald 2.1 m	asm-0086	4.4	2001.19.04	McDonald 0.9 m
mdr023	4.1	1999.10.03	McDonald 2.1 m	sara0082	3.7	2001.21.04	SARA 0.9 m
mdr24a	6.0	1999.11.03	McDonald 2.1 m	tkw-0065	7.3	2001.22.04	McDonald 0.9 m
mdr29a	8.7	1999.15.03	McDonald 2.1 m	sara0086	6.8	2001.24.04	SARA 0.9 m
mdr030	1.5	1999.17.03	McDonald 0.9 m	IAC80A08	0.8	2001.25.04	Teide 0.8 m
mdr033	2.0	1999.19.03	McDonald 0.9 m	sara0088	7.0	2001.25.04	SARA 0.9 m
mdr035	6.0	1999.20.03	McDonald 0.9 m	IAC80A09	6.1	2001.26.04	Teide 0.8 m
mdr039	5.3	1999.23.03	McDonald 0.9 m	sara0089	5.4	2001.26.04	SARA 0.9 m
caf48r1r2	7.5	1999.12.04	Calar Alto 1.2 m	suh-102	3.9	2001.29.04	Suhora 0.6 m
suh-75	1.7	1999.13.04	Suhora 0.6 m	suh-103	0.6	2001.30.04	Suhora 0.6 m
caf48r3	9.3	1999.13.04	Calar Alto 1.2 m	suh-104	0.1	2001.30.04	Suhora 0.6 m
mdr091	4.0	1999.10.12	Fick 0.6 m	IAC80A17	6.1	2001.30.04	Teide 0.8 m
mdr093	6.2	1999.13.12	Fick 0.6 m	mdr198	7.0	2002.17.02	Fick 0.6 m
mdr095	2.4	1999.14.12	Fick 0.6 m	mdr199	1.5	2002.05.04	Fick 0.6 m
mdr096	4.9	1999.16.12	Fick 0.6 m	mdr200	4.5	2002.06.04	Fick 0.6 m
mdr098	2.1	2000.08.02	McDonald 0.9 m	suh-109	1.9	2002.07.05	Suhora 0.6 m
mdr100	1.3	2000.08.02	McDonald 0.9 m	sara141	7.3	2002.07.05	SARA 0.9 m
mdr103	4.6	2000.10.02	McDonald 0.9 m	suh-110	5.4	2002.08.05	Suhora 0.6 m
mdr108	2.7	2000.12.02	McDonald 2.1 m	suh-111	1.2	2002.09.05	Suhora 0.6 m
mdr110	1.0	2000.12.02	McDonald 2.1 m	adg-519	0.7	2002.11.05	Mt. Bigelow 1.5 m
mdr111	3.3	2000.28.02	Fick 0.6 m	suh-112	1.2	2002.12.05	Suhora 0.6 m
mdr112	3.7	2000.01.03	Fick 0.6 m	fe0512oh	2.2	2002.12.05	OHP 1.9 m
mdr113	4.0	2000.02.03	Fick 0.6 m	jr0512	3.4	2002.12.05	Moletai 1.65 m
mdr114	1.5	2000.03.03	Fick 0.6 m	suh-113	4.4	2002.13.05	Suhora 0.6 m
mdr115	6.3	2000.04.03	Fick 0.6 m	jr0513	3.7	2002.13.05	Moletai 1.65 m
mdr116	2.6	2000.04.03	Fick 0.6 m	fe0513oh	1.1	2002.13.05	OHP 1.9 m
mdr117	6.0	2000.05.03	Fick 0.6 m	jgp0209	0.7	2002.14.05	Teide 0.8 m
mdr118	3.3	2000.05.03	Fick 0.6 m	jkt-003	1.7	2002.14.05	JKT 1.0 m
mdr119	3.8	2000.04.05	Fick 0.6 m	jkt-007	5.6	2002.17.05	JKT 1.0 m
mdr120	6.0	2000.05.05	Fick 0.6 m	a0239	1.0	2002.18.05	McDonald 2.1 m
suh-101	6.0	2000.02.11	Suhora 0.6m	jr0518	1.7	2002.18.05	Moletai 1.65 m
suh-102	2.9	2000.03.11	Suhora 0.6m	jr0519	2.4	2002.19.05	Moletai 1.65 m
suh-103	1.4	2000.05.11	Suhora 0.6m	jr0520	2.2	2002.20.05	Moletai 1.65 m
suh-104	9.7	2000.05.11	Suhora 0.6m	jr0521	3.0	2002.21.05	Moletai 1.65 m
suh-105	4.6	2000.07.11	Suhora 0.6 m				

Table 2. Subgroups used in pulsation analysis.

Group	Inclusive dates	Hours of data
I	1998.28.01–1998.01.02	26.7
II	1998.22.11–1998.26.11	10.2
III	1999.06.03–1999.13.04	63.6
IV	1999.10.12–1999.16.12	17.5
V	2000.08.02–2000.05.03	42.4
VI	2000.04.05–2000.05.05	9.8
VII	2000.02.11–2000.22.12	45.7
VIII	2001.18.01–2001.01.02	55.0
IX	2001.19.04–2001.30.04	52.0
X	2002.05.04–2002.21.05	56.8

independently, without using periods detected in other groups. These independent group reductions decrease the likelihood of selecting a daily alias over a real pulsation. Only in our Group X data do we detect a mode (f_2) inconsistent with the other group reductions. As such, we presume that our periods for f_1 – f_5 are not aliases, with the exception of f_2 in Group X, which is a daily alias away from the real period. Frequencies determined for the better data sets are in Table 3 with the corresponding temporal spectra of the best groups (Groups III, V and IX) and the pre-whitened residuals in Fig. 2. Though some signal remains in the Fourier transform after pre-whitening within these groups, we cannot distinguish any remaining pulsation frequencies from noise.

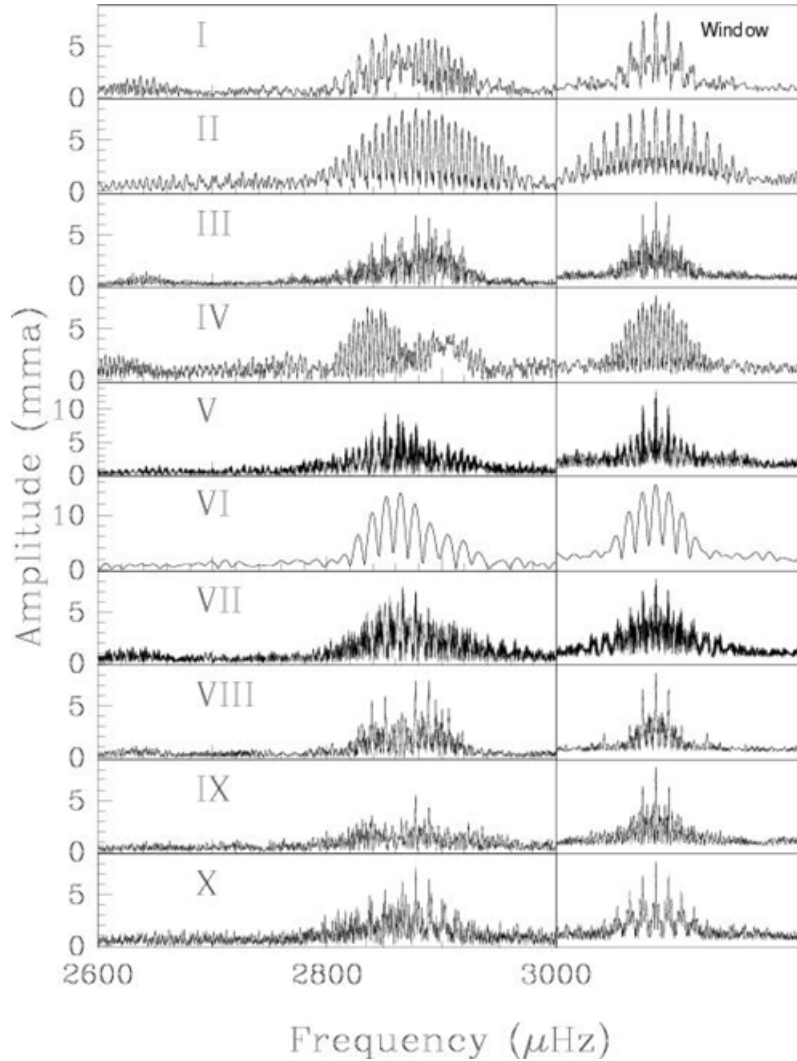


Figure 1. Temporal spectra and window functions of Feige 48 for the groups listed in Table 2.

From our best solution for the Group III data, temporally adjacent groups were added one at a time and frequencies and amplitudes were again fitted until a satisfactory fit was determined for all the data. Though there is still a chance that some modes may be off by an annual or monthly alias, the periods, frequencies and amplitudes in Table 4 represent our best solution. Also indicated by Table 3 are three pulsation periods that appear only within the span of a single group. However, the amplitudes are sufficiently low that some possibility exists that they could be due to noise or aliasing. As such,

we will not include them in our analysis, but we mention them as they are possibly stochastically excited modes within an otherwise stable pulsation spectrum. Note also that an error corresponding to an annual (or even monthly) alias produces only a small change in the period or frequency, and so will not affect the modelling for asteroseismic analysis. Such a mistake, however, would be fatal to the period stability analysis.

Feige 48 shows five distinct and consistent pulsation modes. Four of the stable modes cluster with periods near 350 s and a single mode

Table 3. Comparison of the pulsation frequencies (in μHz) detected in various runs. Formal least-squares errors are provided in parentheses.

Group μHz	f_1	f_2	f_3	f_4	f_5
I†	2636.96(15)		2850.530(40)	2874.40(23)	2877.310(50)
III	2641.98(1)	2837.53(1)	2850.833(4)	2877.157(3)	2906.275(4)
V	2641.49(2)	2837.53(1)	2850.833(3)	2877.177(4)	2890.025(19)
VIII	2642.00(7)	2837.53(5)	2850.818(17)	2877.153(12)	2906.266(22)
IX	2641.98(6)	2837.78(3)	2841.151(9)	2850.946(26)	2877.185(13)
X	2641.86(6)	2826.97(6)*	2850.811(12)	2877.220(10)	2906.665(43)

†These frequencies are directly from K98.

*Indicates modes offset by approximately the daily alias (11.56 μHz).

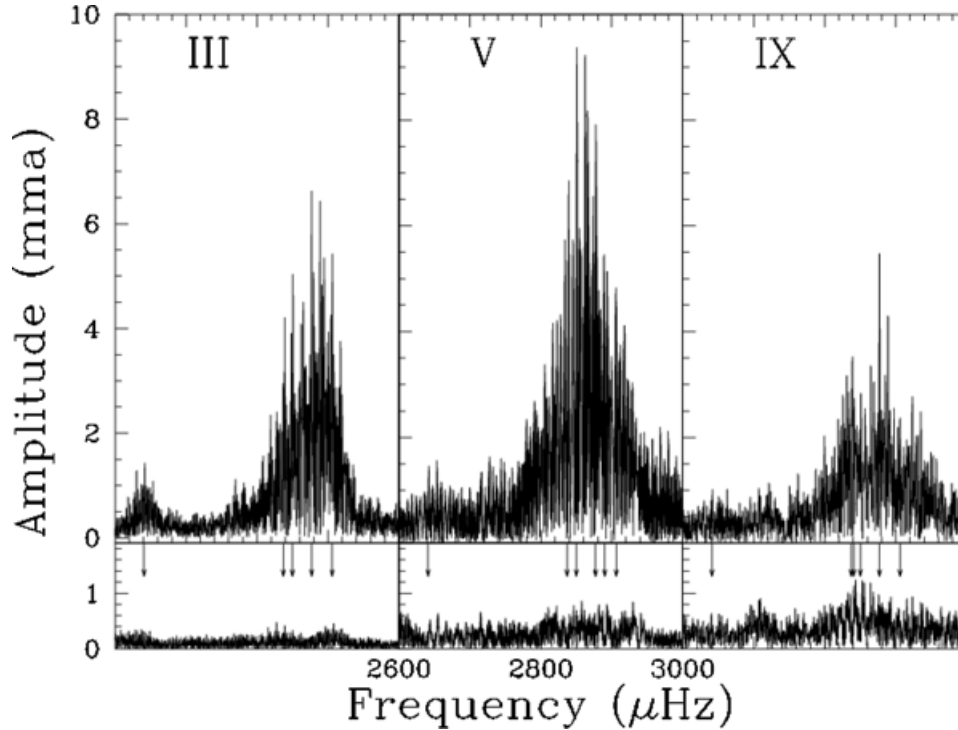


Figure 2. Temporal spectra (top) and residuals after pre-whitening by frequencies in Table 3 (bottom).

Table 4. Least-squares solution to the entire data set. Formal least-squares errors are in parentheses.

Mode	Period (s)	Frequency (μHz)	Amplitude (mma)
f_1	378.502960(37)	2641.98731(23)	1.19(6)
f_2	352.409515(32)	2837.60791(21)	1.30(6)
f_3	350.758148(3)	2850.96729(7)	4.17(6)
f_4	347.565033(19)	2877.15942(4)	6.35(6)
f_5	344.082794(15)	2906.27734(8)	3.57(6)

lies at 378.5 s. The three shortest-period modes also have the highest amplitudes – over three times higher than the two longer-period modes.

Our initial interest in follow-up observations of Feige 48 was amplitude variability observed by K98. Our hope was to detect unresolved pulsations that could be responsible for the apparent amplitude variability they reported. However, it appears that the pulsations are resolved, and each has a variable amplitude of at least 30 per cent. The amplitudes determined for each of our groups for the three high-amplitude modes are shown in Fig. 3. All three amplitudes show change, though only f_3 has a dramatic degree of variability.

4 ANALYSIS OF THE PULSATION SPECTRUM OF FEIGE 48

4.1 Frequency splittings in Feige 48

For most sdBV stars, sufficient data do not exist to resolve the complete pulsation structure. For stars with resolved temporal spectra (Kilkenny 2001) there are typically too many modes to be accounted

for by current pulsation theory unless high ℓ values are included (where, by high ℓ , we mean $\ell \geq 3$). Though higher ℓ modes could be present, such modes suffer from severe cancellation effects across the unresolved stellar disc. In any case, identification of rotationally split multiplets ($\ell = 1$ triplets or $\ell = 2$ quintuplets of nearly equally spaced modes, for example) could aid in accounting for the many modes seen. Unfortunately, previous studies have been limited by a lack of equally spaced (in frequency or period) pulsations as a constraint on the observed ℓ values (with the exception of PG 1605+072; Kawaler 1999).

Even though Feige 48 has a relatively simple pulsation spectrum, understanding why this star pulsates with these frequencies still presents a problem. The tight cluster of four modes with periods spanning a range of less than 10 s is impossible to accommodate with purely radial pulsation modes in sdB models. Even appealing to non-radial pulsations, the closeness of these periods means that rotation (or other departures from spherical symmetry) must play a role. The reason is that if all are $m = 0$ modes, standard evolutionary models of sdB stars at the same T_{eff} and $\log g$ as Feige 48 do not have dense enough frequency spectra to account for these four modes, even if one appeals to modes of higher degree than $\ell = 3$.

However, Feige 48 may provide important clues in its observed pulsation spectrum. The frequency difference between f_3 and f_4 (26.2 μHz) is very close to the difference between f_4 and f_5 (29.1 μHz). Though not exact, this splitting is highly suggestive that f_3 , f_4 and f_5 are a rotationally split mode, and probably $\ell = 1$. We note that the frequency splitting is not precisely equal (26 versus 29 μHz). First-order pulsation theory (if applicable here) says that the splitting should be precisely equal – though observations of rotational splitting in white-dwarf stars show asymmetries such as this (i.e. in PG 2131+066, Kawaler et al. 1995 or GD358, Winget et al. 1994). Such asymmetries can be caused by many higher-order processes including rotation and magnetic fields. However this mainly observational paper is not the medium for

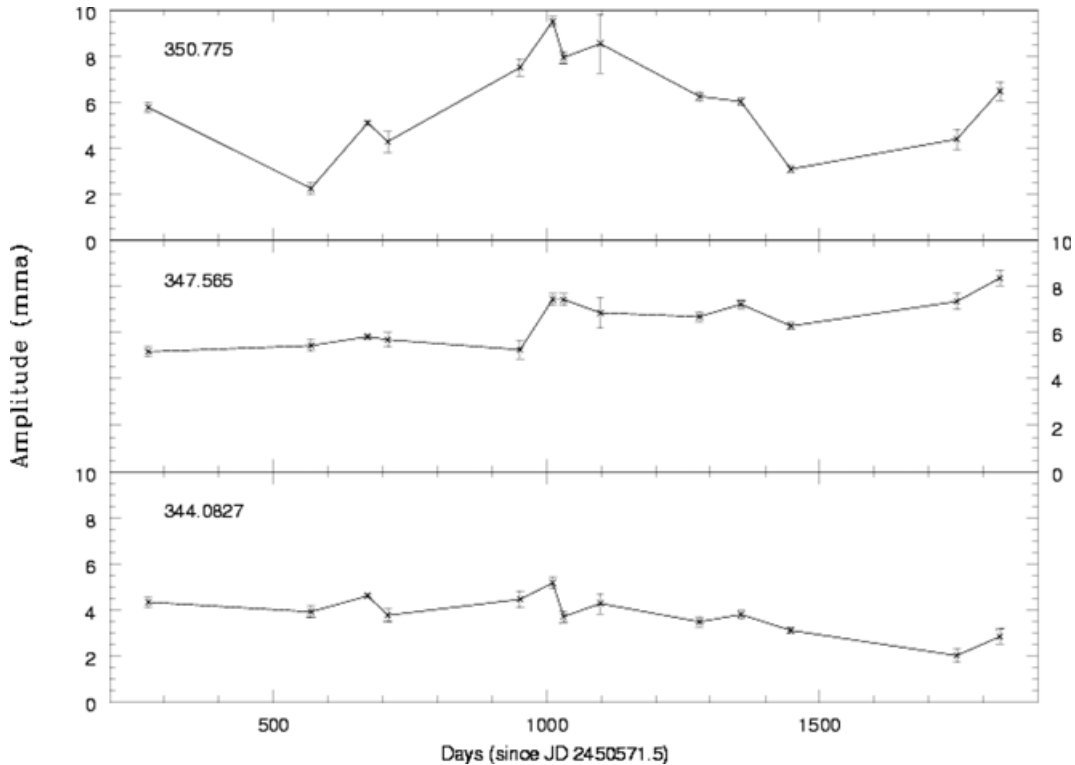


Figure 3. Pulsation amplitudes for the three largest-amplitude modes.

such a discussion, so we will ignore the small departures from symmetry.

Another possible clue is that the spacing between f_2 and f_3 is $13.2 \mu\text{Hz}$, which is almost exactly half the frequency spacing between f_3 and f_4 . Thus we could interpret the observed frequencies as follows: the f_3, f_4, f_5 set make an $\ell = 1$ triplet, meaning the model needs to fit f_4 with an $\ell = 1$, and f_3 and f_5 reveal the rotation rate. Or, f_2, f_3 and f_4 are three components of an $\ell = 2$ quintuplet with a spacing of $13.2 \mu\text{Hz}$. In this case the $m = 0$ component could either be f_3 itself or $f_3 + 13.2 \mu\text{Hz}$ (with a period of 349.1 s).

4.2 Comparison with standard evolutionary models

Though we have by no means a complete grid of models and cannot quantify the uniqueness of our results, we can see if either of the above possibilities is consistent with expectations from standard evolutionary models of sdB stars. We take the approach of Kawaler (1999): create several series of evolutionary models that pass through the spectroscopic error box of T_{eff} and $\log g$, being sure to sample several regions. From these grids, we search for periods near those observed, creating a list of models and pulsation periods. From within this list, we further constrain the match using the required values of ℓ and m for each possible interpretation of the splittings noted above. For the best model series, we create models with smaller evolutionary steps, finding the one with the best fit to the periods.

With five frequencies available, there are multiple ways to match observations with model frequencies depending on the assumed values of ℓ and m for each mode. The most obvious assumption to make is that modes f_3, f_4 and f_5 form a rotationally split triplet with $\ell = 1, m = -1, 0, +1$. This choice has no ‘missing members’ of the multiplet. With this assumption, the model that fits the spectroscopic

data must show an $\ell = 1$ mode at f_4 , and modes at f_1 and f_2 . Other choices for this triplet which *do* require that some components of the multiplet which are unobserved are $\ell = 2$, with $\Delta m = 2$ ($m = -2, 0, +2$) or $\Delta m = 1$ (e.g. $m = -2, -1, 0$ or $m = -1, 0, +1$). Similarly, the interpretation of f_2, f_3 and f_4 being components of an $\ell = 2$ multiplet, as described above, is viable.

Without choosing a priori one of these interpretations, we examined evolutionary models within our preliminary grid as described below. We generated full evolutionary stellar models using a version of the ISUEVO stellar evolution program (Dehner & Kawaler 1995; Dehner 1996; Kawaler 1999) that incorporates semiconvection in the core helium-burning phase. Our initial grid of evolutionary tracks and models spans the observed range of T_{eff} and $\log g$ for sdB stars with a core mass of $0.47 M_{\odot}$ and solar metallicity. We computed evolutionary tracks for models with hydrogen envelope masses ranging from 0 to $0.00550 M_{\odot}$. From this initial grid, we focused on model series whose evolutionary tracks pass within 1σ of the spectroscopically determined values of T_{eff} and $\log g$ (HRW). For these models, we then calculated their pulsation periods to see which (if any) had radial or non-radial pulsation periods near those observed, for any possible choice of ℓ and identification of the $m = 0$ component of a rotationally split multiplet. For the sequence that most closely matched the observed periods, we iteratively produced models with smaller differences in H shell masses and smaller evolutionary time-steps.

We did find a model that matched the spectroscopic constraints, and, with an ad hoc rotational splitting of $27.73 \mu\text{Hz}$ (the average of the observed splittings), could explain four of the five observed frequencies. The closest model fit came from a model in the evolutionary track shown in Fig. 4. This model does an excellent job in explaining f_2 – f_5 and requires the identification of f_3, f_4 and f_5 as a rotationally split $\ell = 1$ triplet. The model is fairly evolved (as

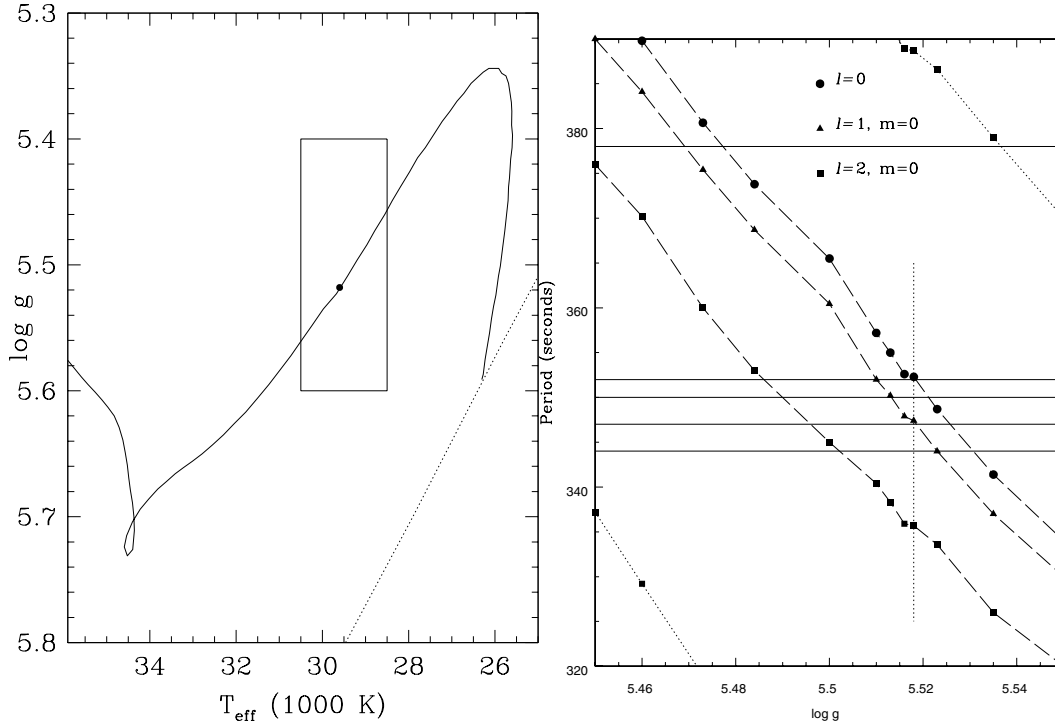


Figure 4. Comparison of the model with the observations. The left panel shows the evolutionary model track (solid line) containing our best-fitting model (dot). The dashed line is the ZAHB and the rectangle is the spectroscopic 1σ error box. The right panel compares the model periods (points) to those observed (solid lines). The vertical dashed line indicates the best-fitting model.

Table 5. Comparison of observations with our best-fitting evolutionary model.

Number	Frequency μHz	Period (s)		Model		
		Star	Model	n	l	m
1	2641.99	378.5026	(374)	(5)	(3)	(0)
2	2837.60	352.4105	352.2550	0	0	0
3	2850.83	350.7750	350.7777	1	1	-1
4	2877.16	347.5650	347.3991	1	1	0
5	2906.28	344.0825	344.0850	1	1	+1

	Mass	H shell mass	T_{eff}	$\log g$
Spectroscopy			29500 ± 300 K	5.50 ± 0.05
Model	0.4725	0.0025	29635	5.518

we suspected) and has nearly exhausted its core helium, with only 0.74 per cent (by mass) of the core composed of helium. Table 5 show a comparison between the observed periods and best-fitting model periods, and the observed spectroscopic properties and the model parameters. This model fits all but the lowest frequency to a precision of better than 0.2 s. The model temperature agrees to within 150 K, and $\log g$ agrees to within 0.02 dex of the measured values; these are well within the 1σ uncertainties quoted by HRW.

Despite the perception that there are many degrees of freedom, this procedure produced only one model series that fitted the observations: i.e. no models had appropriate $\ell = 2$ or $\ell = 1, n = 2$ periods. Of course, as we do not have model grids covering all parameter space, it is possible that another model, with perhaps a different core mass or metallicity, may fit better or have altogether different ℓ identifications. This procedure also failed to produce a model that could

explain all five observed frequencies in terms of normal modes and rotational splitting. Though the model does produce an $\ell = 3, m = 0$ mode at the 378-s period, which is near the observed 378-s mode, we currently find no evidence to suggest that Feige 48 has $\ell > 2$. As such, we must confess that our model does not reproduce this period without appealing to high ℓ . Without further evidence (such as other observed members of the multiplet) for invoking high- ℓ modes, we are forced to leave $f1$ as unmatched by our model. Additionally, any $\ell = 2$ matches fitted less observed periods. Since we do not have a complete sample of models and this is really just an illustrative example, we are not alarmed. However, it could also indicate that our current models do not include enough physics to be accurate.

The pulsation results for the closest-fitting modes in our best-fitting model series are shown in Fig. 4. Even a small change in $\log g$ (as an indication of age) of 0.005 dex changes the calculated periods by more than 3 s, worsening the fit to the observations. Likewise, a change in the envelope layer thickness quickly destroys the fit by moving the path of the evolutionary track away from the spectroscopic error box. As the right panel of Fig. 4 shows, within this period space, model periods are relatively uncrowded. Overtones are separated by ~ 100 s for $\ell = 0$ and 1 modes, and ~ 50 s for $\ell = 2$ modes. Overtones for $\ell = 2$ do appear in the top-right and lower-left of the figure.

4.3 Testing the mode identifications

A test of our (or any) model is the measured constraint on rotational velocity. The observed average rotational splitting of $27.7 \mu\text{Hz}$ imposed on our $\ell = 1$ model identification implies a rotation period of 0.42 d (10 h). With a radius of $0.20 R_{\odot}$, this model has an equatorial rotation velocity of 24 km s^{-1} . To match the constraints of HRW ($v \sin i \leq 5 \text{ km s}^{-1}$) requires $i \leq 12^{\circ}$. If we use the less restrictive

value determined by HRW for only the unblended spectral lines in Feige 48 of $v \sin i \leq 10 \text{ km s}^{-1}$, our inclination limit increases to $i \leq 25^\circ$.

The identification of an $\ell = 1$ triplet and a radial mode suggest an observation that can be used to test the model. As in white dwarfs (Kepler et al. 2000), time-series spectroscopy (particularly in the ultraviolet) should present an effective means of distinguishing between low- and high-order (ℓ) non-radial pulsations. Though it is still in its infancy for sdBV stars (O’Toole et al. 2002; Woolf, Jeffery & Pollacco 2002), if the 378-s period is $\ell = 3$, it should be obvious in ultraviolet (UV) spectroscopy (perhaps less so in the optical), where it should have a significantly higher amplitude than at optical wavelengths. The same is true for our identification of the $\ell = 1$ triplet. If any member of our identified triplet really has a different ℓ value, the wavelength dependence of its amplitude will be different. Such a test should be obtained as an independent confirmation of our $\ell = 1$ determination. While this test can be applied to any sdBV star, Feige 48 has comparatively long pulsation periods (exceeded only by PG 1605+072) and its rather simple temporal spectrum (only five periods compared to 55 for PG 1605+072) make it an ideal candidate for time-series spectroscopic study.

5 STABILITY OF THE PULSATION PERIODS

As a star evolves, the pulsation properties evolve in response. In the case of the subdwarf B stars, evolutionary models indicate that they reside on or near the ZAHB for approximately 10^8 yr. Upon exhausting their core helium supply, they leave the hori-

zontal branch (HB), their $\log g$ goes down, and pulsation periods lengthen. The time-scale for evolutionary pulsation period changes (\dot{P}/P) after leaving the HB is about 10 times faster than while on the HB.

If Feige 48 has a comparatively small $\log g$ because it is a mature HB star that has left the ZAHB, we expect Feige 48 to have an evolutionary \dot{P} smaller than PG 1605+072, yet larger than for shorter-period pulsators. Since PG 1605+072 does not appear to have pulsations stable enough for an analysis of secular period change caused by evolution (Reed 2001), Feige 48 is the best candidate to examine the e -folding time for structural changes caused by its core evolution. As a guide, the model described in Section 4 has $\dot{P} = 1.714 \times 10^{-5} \text{ s yr}^{-1}$. With about three years of usable data, the phase of a 350-s period should change by ~ 14 s in that time. This is close to our limit of detection.

To examine long-term phase change, we followed the methods outlined in Winget et al. (1985) and Costa & Kepler (2000). First, we obtain a best-fitting least-squares fit to all of the periodicities present over the entire span of the observations (Table 4). We then fix the frequencies at these best-fitting values, and recompute the pulsation phases (again via least squares) for each group in Table 2 (note that Groups III and V were divided into two sub-groups each because of the long length of the runs). This computed phase represents the observed time of maximum (O) for that group, which differs from the computed time (C) from the fit to all data. The resulting $O-C$ diagram is shown in Fig. 5 for the three highest-amplitude modes (with the pulsation period indicated in each panel). The phase zero point is that defined in K98 as JD = 2450571.50.

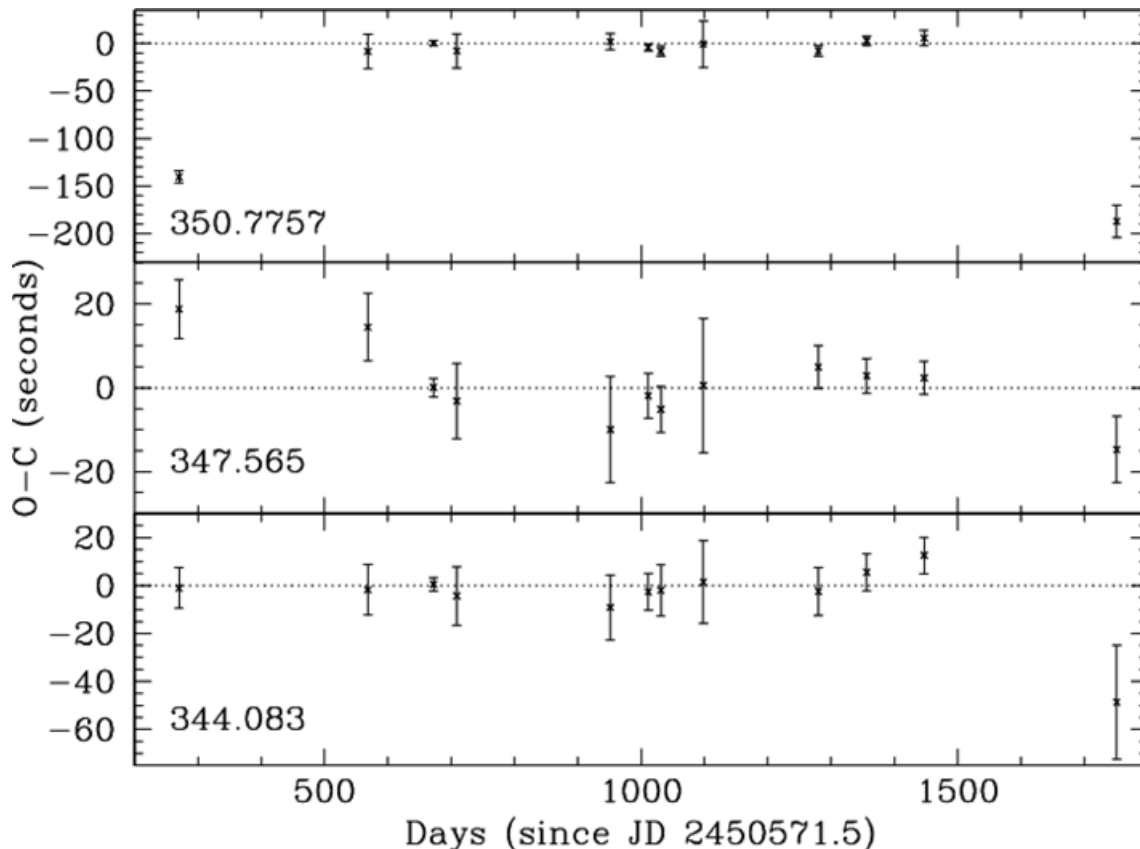


Figure 5. $O-C$ diagrams for the three largest-amplitude modes.

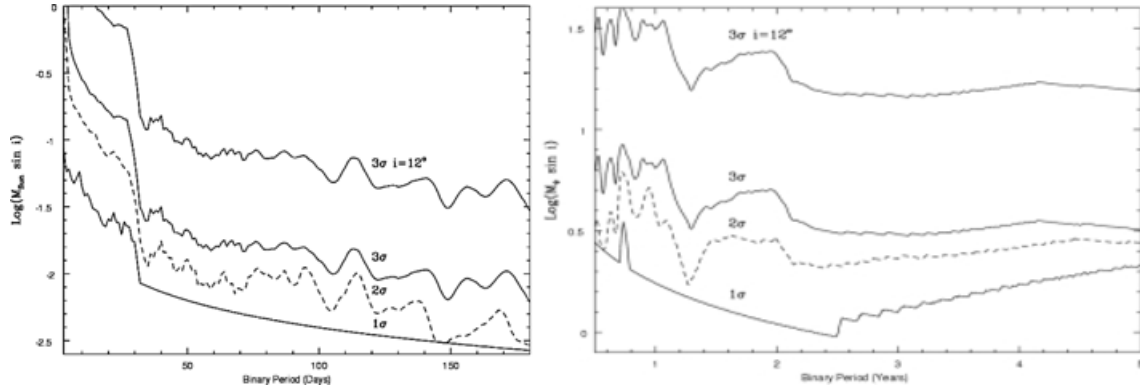


Figure 6. 1σ , 2σ (dashed line) and 3σ upper limits on companions to Feige 48. The time axis is continuous between panels, but changes scale from days to years. The mass axis is discontinuous between panels as the left panel is in solar masses and the right panel has units of Jupiter masses.

Fig. 5 shows that the phases are stable throughout most of our observations. Until the Group X data were collected, we believed the Group I data suffered a timing error (proposed in K98). However, it now seems apparent that the pulsation modes were only stable over a limited time-span (from Groups II–IX). As a check, we analysed various subgroups of Group X data and reproduced the same phase result. Such a problem is observed in other sdBV stars over a much shorter time-scale (Reed 2001). Though we are disappointed in the apparent lack of phase stability, we still have an approximately three-year span of phase-stable observations. We therefore used the phase-stable data to place upper limits on the magnitude of \dot{P}/P . The combined $O-C$ data of the three highest-amplitude modes were weighted and fitted using least squares and give $\dot{P}/P = 4.9 \pm 5.3 \times 10^{-16} \text{ s}^{-1}$. The data are therefore consistent with zero period change and provide a 1σ lower limit on an evolutionary time-scale of $3.1 \times 10^7 \text{ yr}$. Of course evolution is not the only thing that can drive period changes (see for example Paparó et al. 1998). However, evolutionary models predict that sdBV periods should change in a predictable way (increasing just off the ZAHB, then decreasing after core helium exhaustion, and finally increasing again during shell helium fusion). By measuring \dot{P} for several sdBV stars at different stages, we should be able to determine if evolution (as predicted) is driving the period changes.

5.1 $O-C$ variations from reflex orbital motion – planets around Feige 48?

With the phase-stable portion of the data, we can also place useful limits on companions to Feige 48. Orbital reflex motion would create a periodic shift in the arrival time of the pulsation, which would be observed in pulsation phase. Thus any companion must create a periodic phase change within our $O-C$ uncertainties over a scale of days to years.¹ To place limits on companions, we calculated companion mass as a function of binary period and semimajor axis by fitting sine curves (for circular orbits) within our 1 , 2 , and 3σ $O-C$ limits. To ensure an upper limit ($M \sin i$) on reflex motion, we use the ‘noise’ in the FT of our $O-C$ as a 1σ lower limit. This results in a minimum phase shift of 5 s for binary periods under 20 d and 4 s for longer periods. Fig. 6 graphically presents our sensitivity to orbital companions. The top line represents the 3σ limit for $i = 12^\circ$ (our

model constraint). In the short-period case (periods under 30 d), the constraint is the limit imposed by the phase errors of individual runs within the data; in the long-period case it is the flatness of the $O-C$ diagram (including the errors of combined runs) over the phase-stable region of our observations. The drop at 30 d corresponds to the change from $O-C$ values determined for single runs to group data sets.

Feige 48 is a horizontal-branch star that has lost considerable mass between the red-giant branch and its current evolutionary state. Any companion separated by more than $\sim 1 \text{ au}$ is far enough away that common-envelope evolution (or vaporization) has been avoided. In addition, the orbital separation will have roughly doubled as Feige 48 lost approximately half its mass during the red-giant phase. This should produce two cases for binaries:

- (i) Close stellar companions with original separations $\leq 1 \text{ au}$ will produce a short-period binary (which have periods on order of weeks or less) after a common envelope phase.
- (ii) Companions distant enough to avoid a common envelope phase (or vaporization) will have orbital periods on the order of a year or more.

The two panels of Fig. 6 reflect this duality (though it does cover all periods between 2 d and 5 yr).

The left panel of Fig. 6 indicates our limits on stellar companions. Our 1σ limit is less than $0.1 M_\odot \sin i$ for a binary period of 3 d. The right panel shows our limits on substellar companions. Our ‘average’ 3σ limit for $i = 12^\circ$ is $\approx 12 M_\psi$, while our best 1σ limit would detect Jupiter at a period of 2.5 yr. Our data are currently sensitive enough to detect extrasolar ‘warm Jupiter’ type planets² at a distance of 0.6–3.0 au. Planets with orbital separations less than $\sim 1 \text{ au}$ would not have survived the red-giant phase. Our data do not rule out a companion in an extremely short-period binary or at low inclination.

6 CONCLUSIONS

From our multiseason photometry of Feige 48, we have consistently detected five pulsation periods. Of these five, three ($f1$, $f3$ and $f4$) are consistent with K98. One frequency ($f5$) differs by a daily alias, while the fifth frequency (2874 μHz) of K98 is not detected in our

¹ We assume we could detect an orbital period up to twice our observed time-base.

² A complete list of extrasolar planets is maintained at <http://www.obspm.fr/encycl/catalog.html>.

data. In data sets V and IX, we also detect new pulsation frequencies at 2890 and 2843 μHz , respectively, indicating that there may be some stochastically excited pulsations in Feige 48. This is consistent with pulsation behaviour seen in another sdBV star, PG 1605+072 (Reed 2001).

Our attempted model fit follows the strategy that has been successfully applied to other classes of pulsating stars, but has rarely worked for sdBV stars; namely using observed frequency splittings to impose ℓ constraints on models. Using standard evolutionary models, our preliminary model grid includes a model that is able to explain all but the lowest-frequency stable pulsations. Most exciting is the fact that such standard models fail to explain all five frequencies. Thus, despite its relative simplicity and the richness of the parameters available, the failure of this model suggests that standard stellar evolution theory does not fully explain the evolution of sdB stars or the nature of pulsations within them. We have something new to learn.

Our modelling example shows that Feige 48 should also serve as an interesting test for other methods of mode identification. Though optical multicolour photometry was not useful for identifying pulsation modes in KPD2109+4401 (Koen 1998), we expect that UV multicolour photometry as developed by Robinson et al. (1995), will be useful to determine if high-order ℓ modes are present in sdBV stars (as indicated by Billères et al. 2000; Brassard et al. 2001). The argument for high-order ℓ values is particularly interesting in light of the frequencies detected in the data of Group V. If the lowest-frequency mode is disregarded, the remaining modes have frequency spacings of 13.3, 26.4, 12.8 and 16.3 μHz respectively. If these were all parts of a single, rotationally split mode, it would require $\ell \geq 3$. Such an ℓ value should be apparent in UV multicolour photometry (see, for example, Kepler et al. 2000). As such, we look forward to the analysis of data from the *Hubble Space Telescope* obtained by Heber (2002, private communication). Should Heber's (2002, private communication) data from the *Hubble Space Telescope* agree with our $\ell = 1$ interpretation, Feige 48 would make an excellent star to calibrate other mode identification methods in sdBV stars, such as optical time-series spectroscopy (O'Toole et al. 2002; Woolf et al. 2002).

The results of our $O-C$ analysis are consistent with a non-binary nature for the star within the data limits. They also indicate that using the $O-C$ diagram to detect planets around evolved stars is possible, though in this case we did not detect any. We plan to continue to monitor Feige 48 over the next several years to tighten the constraints on planetary companions.

Our limit on a stellar companion also addresses the origin of sdB stars. Binary evolution is a candidate for producing sdB stars, either through common-envelope evolution (Green, Liebert & Saffer 2001; Sandquist, Taam & Burkert 2000) or via Roche-lobe overflow near the tip of the red-giant branch (Green et al. 2000). Though observations indicate that a great many sdB stars are in binaries (Green et al. 2001; Han et al. 2002), the evolutionary sequence that produces sdB stars is independent of binary evolution (D'Cruz et al. 1996), is bimodal, or has several paths that can result in the production of an sdB star (perhaps including the merger of two low-mass white dwarfs as described by Iben & Tutukov 1986). For the case of Feige 48, it would appear that it is either in a short-period binary (whose orbital period is commensurate with the ~ 10 -h rotation period predicted with our model), in a long-period binary with an orbital period substantially longer than our data (which would rule out Roche-lobe overflow, so the companion would have no effect on the evolution of the pre-sdB

star), in a binary with an extremely low inclination, or a single star.

ACKNOWLEDGMENTS

MDR was partially funded by NSF grant AST9876655 and by the NASA Astrophysics Theory Program through grant NAG-58352 and would like to thank the McDonald Observatory TAC for generous time allocation. SD, SLS and JLD (Visiting Astronomers at the German-Spanish Astronomical Centre, Calar Alto, operated by the Max-Planck-Institut for Astronomy, Heidelberg, jointly with the Spanish National Commission for Astronomy) acknowledge travel grant DR 281/10-1 from the Deutsche Forschungsgemeinschaft. PM is supported in part by Polish KBN grant 5 P03D 012 020. A. Ulla acknowledges financial support from the Spanish Ministry of Science and Technology under grant AYA2000-1691. The IAC80 0.8-m telescope is operated in the Spanish Observatorio del Teide (Tenerife) by the Instituto de Astrofísica de Canarias.

REFERENCES

- Billères M., Fontaine G., Brassard P., Charpinet S., Liebert James, Saffer R. A., 2000, *ApJ*, 530, 441
 Brassard P., Fontaine G., Billères M., Charpinet S., Liebert James, Saffer R. A., 2001, *ApJ*, 563, 1013
 Charpinet S., Fontaine G., Brassard P., 2001, *PASP*, 113, 775
 Costa J. E. S., Kepler S. O., 2000, *Baltic Astron.*, 9, 451
 D'Cruz N. L., Dorman B., Rood R. T., O'Connell R. W., 1996, *ApJ*, 466, 369
 Dehner B. T., 1996, PhD dissertation, Iowa State University
 Dehner B. T., Kawaler S. D., 1995, *ApJ*, 445, 141
 Feige J., 1958, *ApJ*, 128, 267
 Green E. M., Liebert J., Saffer R. A., 2001, in Provençal J. L., Shipman H. L., MacDonald J., Goodchild S., eds, *Proc. 12th European Conference on White Dwarfs*. Astron. Soc. Pac., San Francisco, p. 192
 Green R. F., Schmidt M., Liebert J., 1986, *ApJ*, 61, 305
 Han Z., Podsiadlowski Ph, Maxted P. F. L., Marsh T. R., Ivanova N., 2002, *MNRAS*, 336, 449
 Heber U., Reid N. I., Werner K., 1999, *A&A*, 348, L25
 Iben I., Jr, Tutukov A. V., 1986, *ApJ*, 311, 753
 Kanaan A., O'Donoghue D., Kleinman S. J., Krzesinski J., Koester D., Dreizler S., 2000, *Baltic Astron.*, 9, 387
 Kawaler S. D., 1999, in Solheim J. E., Meistas E. G., eds, *Proc. 11th European Workshop on White Dwarfs*. Astron. Soc. Pac., San Francisco, p. 158
 Kawaler S. D. et al. (the WET Collaboration), 1995, *ApJ*, 450, 350
 Kepler S. O., Robinson E. L., Koester D., Clemens J. C., Nather R. E., Jiang X. J., 2000, *ApJ*, 539, 379
 Kilkenny D., 2001, in Aerts C., Bedding T. R., Christensen-Dalsgaard J., eds, *Proc. IAU Coll. 185, Radial and Nonradial Pulsations as Probes of Stellar Physics*. Astron. Soc. Pac., San Francisco, p. 356
 Kleinman S. J., Nather R. E., Phillips T., 1996, *PASP*, 108, 356
 Koen C., 1998, *MNRAS*, 300, 567
 Koen C., O'Donoghue D., Pollacco D. L., Nitta A., 1998, *MNRAS*, 300, 1105
 O'Brien M. S. et al. (the WET collaboration), 1998, *ApJ*, 495, 458
 O'Donoghue D., Koen C., Kilkenny D., Stobie R. S., Lynas-Gray A. E., 1999, in Solheim J. E., Meistas E. G., eds, *Proc. 11th European Workshop on White Dwarfs*. Astron. Soc. Pac., San Francisco, p. 149
 O'Toole S. J., Bedding T. R., Kjeldsen H., Dall T. H., Stello D., 2002, *MNRAS*, 334, 4710
 Paparó M., Saad S. M., Szeidl B., Kolláth Z., Abu Elazm M. S., Sharaf M. A., 1998, *A&A*, 332, 101

Reed M. D., 2001, PhD dissertation, Iowa State University

Reed M. D., Kawaler S. D., Kleinman S. J., 2000, in Szabados L., Kurtz D. W., eds, Proc. IAU Coll. 176, The Impact of Large-Scale Surveys on Pulsating Star Research. Astron. Soc. Pac., San Francisco, p. 503

Robinson E. L. et al., 1995, ApJ, 438, 908

Sandquist E. L., Taam R. E., Burkert A., 2000, ApJ, 533, 984

Winget D. E., Robinson E. L., Nather R. E., Kepler S. O., O'Donoghue D., 1985, ApJ, 292, 606

Winget D. E. et al. (the WET collaboration), 1994, ApJ, 430, 839

Woolf V. M., Jeffery C. S., Pollacco D. L., 2002, MNRAS, 332, 34

This paper has been typeset from a $\text{\TeX}/\text{\LaTeX}$ file prepared by the author.